

## POLYETHYLENE OXIDES

### Analysis of tablet formation and properties of the resulting tablets

Katharina M. Picker-Freyer\*

Martin-Luther-University, Halle-Wittenberg Institute of Pharmaceutical Technology and Biopharmacy  
Wolfgang-Langenbeck-Str. 4 06120, Halle/Saale, Germany

The aim of this study was to study tablet formation of polyethylene oxides (PEOs) with different molecular masses by means of 3D modeling and comparing the results to those of other more traditional techniques, such as Heckel analysis, analysis by the pressure-time function and energy analysis. The molecular masses ranged between 400,000 and 7,000,000 Da. Material properties, such as water content, particle size and morphology, and glass transition temperature were also studied. To complete this study, elastic recovery dependent on maximum relative density and time were determined. Furthermore, the crushing force of the tablets and their morphology were analyzed.

The PEOs consist of smooth edged particles of irregular shape; the particle size is similar to one type of MCC, namely Avicel PH 200. The PEOs are much more ductile during compression than MCC. Elastic recovery after tableting is higher than that for tablets made from MCC and continues for some time after tableting. The crushing force of the resulting tablets is low. In conclusion, with regards to direct compression the PEOs do not appear to be useful as sole tableting excipients.

**Keywords:** compactibility, compression, 3D model, elastic recovery, morphology, polyethylene oxides

## Introduction

Polyethylene oxides (PEOs) have recently been tested for their use as controlled release dosage forms, and hydrophilic matrix tablets as well as extrudates have been successfully produced [1–5]. These studies have shown release characteristics dependent on molecular mass and drug loading. The release is controlled by the extent and rate of swelling of the polymers and zero-order release can be achieved. Furthermore, the PEOs were able to stabilize amorphous indomethacin in tablets [6]. In order to achieve this, mixtures of different molecular mass PEOs with indomethacin were tableted and the recrystallization of the drug was studied by FT-Raman spectroscopy. The results showed recrystallization inhibition by the PEOs which is caused by stabilizing bondings between the drug and polymer.

The application of PEOs as tableting excipients is all the more desirable since PEO is nontoxic and biodegradable. It is a synthetically produced polymer, which results from the polymerisation of ethylene oxide. Chemically this product is known as polyethylene glycol, however, products with a molecular mass of more than 20,000 Da are called PEO [7, 8]. The molecular mass can be as high as 8,000,000 Da. PEO molecules are produced with the aid of catalysts, such as red iron oxide and activated aluminum. In order to achieve PEOs of different molecular masses, the mol-

ecules which are produced are split while under the influence of UV irradiation.

The PEOs are partially crystalline (about 50% [8], between 57 and 85% [9]) and it must be noted here that crystallinity decreases with increasing molecular mass [8, 9]. The glass transition temperature  $T_g$  was determined to be  $-52^\circ\text{C}$  for materials with a molecular mass of several million Da, the  $T_g$  was  $-17^\circ\text{C}$  for a molecular mass of 6.000 Da and the melting point was determined at  $65^\circ\text{C}$  [7, 8, 10].

Despite their usefulness in producing tablets with desired release characteristics or their ability to stabilize amorphous indomethacin in tablets, the powder and tablet deformation properties of the PEOs have been rarely studied. PEOs possess an excellent flowability [9, 11], which is a main factor in high speed tablet production. Furthermore, they showed a high compressibility coupled with a high elastic recovery after tableting. According to [9], no differences between different molecular masses (200,000–7,000,000 Da) could be determined using the Heckel analysis.

Recently, the 3D modeling technique has been introduced to study tablet formation more precisely. The method has been successful in characterizing materials with very different deformation mechanisms, as well as, those with similar deformation mechanisms [12–14].

\* katharina.picker-freyer@pharmazie.uni-halle.de

Thus, the aim of the study is to apply this technique to PEO tablet formation characterization and compare it to other more traditional techniques such as, Heckel analysis, analysis by the pressure-time function and energy analysis. To have a reliable basis for discussion and a comparison of values, MCC with a similar particle size (Avicel PH 200) was used as a kind of inner standard. To evaluate the influence of molecular mass on deformation, five different PEOs with a molecular mass ranging from 400,000 to 7,000,000 Da have been chosen for this study. In order to complete the study, in addition to deformation properties, the powder technological properties and the properties of the final tablets will be described.

## Experimental

### Materials

The five PEOs with different molecular masses, Polyox<sup>®</sup> WSR-N-3000 (P3000, Lot # 483138), Polyox<sup>®</sup> WSR-1105 (P1105, Lot # 481165), Polyox<sup>®</sup> WSR-N-60K (P60K, Lot # 46825), Polyox<sup>®</sup> WSR-301 (P301, Lot # 322468), Polyox<sup>®</sup> WSR-303 (P303, Lot # 155836) were obtained from Union Carbide Inc. (Danbury, CT, USA). The molecular mass of the five PEOs is given in Table 1. For comparison microcrystalline cellulose, MCC, Avicel<sup>®</sup> PH 200 (Avi 200, Lot # 11939 C) from FMC Europe N.V. (Brussels, Belgium) was used.

### Instrumental methods

#### Test conditions

All materials and tablets were equilibrated, produced and stored between 35 and 45% RH. Tableting was performed in a special climate controlled room which was set at  $23 \pm 1^\circ\text{C}$  and  $45 \pm 2\%$  RH.

#### Sorption isotherms

Sorption isotherms were recorded gravimetrically after equilibration at 32% RH. In a preliminary experiment it was proven that equilibration was reached after four days. The powder was equilibrated at a specific relative humidity (RH) over saturated salt solutions [15] for seven days in triplicate. After equilibration the powder was weighed and transferred to the next higher RH for equilibration. This procedure started at 32% RH and in order to avoid any drying influence on sorption and to analyze the sorption of the powder as it was received. It was performed up to 90% RH. Following that, the powder moved to the next lower RH up to 0% RH (phosphorous pentoxide). The water content for each

RH was calculated using the mass of the dry powder as determined at 0% RH.

#### Water content

The water content of the materials used in this study was determined by thermogravimetric analysis using TGA 209 (Netzsch Gerätebau GmbH, Selb, Germany) in triplicate. The powder was heated with  $10 \text{ K min}^{-1}$  up to  $150^\circ\text{C}$  and water loss was determined.

#### Particle size determination

Particle size distribution was analyzed by laser light diffractometry using a dry feeder (Sympatec Rodos 12 SR, Sympatec, Remlingen, Germany; pressure: 4 bar, injector beneath pressure: 60 mbar, focal distance 200 mm and measuring time: 25–35 s) in triplicate. The mean volume particle size distribution was calculated and the median diameter of this distribution was determined. In addition, for the median diameter standard deviation was determined from the raw data.

#### Scanning electron microscopy

Both the powder and tablets were analyzed with the use of scanning electron microscopy (SEM) (JSM 6400, JEOL, Tokyo, Japan) at an accelerating voltage of 15 kV. Before analysis they were mounted onto a sample holder and coated with coal/gold/coal (Balzers, Liechtenstein, Typ SCD 050).

#### Apparent particle density

The apparent particle density of all of the materials was determined by Helium pycnometry (Accupyc 1330, Micromeritics, Norcross, GA, USA) in triplicate. The equilibrated materials were used for analysis in order to determine the apparent particle density at equilibrium conditions; the method has been described by Picker and Mielck [16].

#### Bulk and tap density

Bulk and tap density were determined in triplicate in a weighed 250 mL cylinder using a volumeter (Erweka GmbH, Heusenstamm, Germany). 100 g of the powder was gently filled into the cylinder. Bulk volume was read and bulk density calculated. Following that step, the cylinder was tapped at least 2500 times up to constant volume. Tap volume was read and tap density calculated, and mean and standard deviations were determined.

**Table 1** Powder technological properties of five different PEOs compared to MCC (Mean  $\pm$  SD)

Material	Quality	Molecular mass/Da	Water content, mass/mass/%	Medium particle size/ $\mu\text{m}$	Apparent particle density/ $\text{g cm}^{-3}$	Bulk density/ $\text{g cm}^{-3}$	Tap density/ $\text{g cm}^{-3}$	Carr index/%
PEO	Polyox WSR-N-3000	400000	0.33 $\pm$ 0.01	145 $\pm$ 1	1.248 $\pm$ 0.003	0.528 $\pm$ 0.004	0.611 $\pm$ 0.003	13.69 $\pm$ 0.36
PEO	Polyox WSR-N-1105	900000	0.32 $\pm$ 0.08	145 $\pm$ 1	1.244 $\pm$ 0.002	0.536 $\pm$ 0.004	0.632 $\pm$ 0.004	13.93 $\pm$ 0.98
PEO	Polyox WSR-N-60K	2000000	0.30 $\pm$ 0.17	135 $\pm$ 1	1.245 $\pm$ 0.001	0.497 $\pm$ 0.005	0.567 $\pm$ 0.005	12.33 $\pm$ 1.52
PEO	Polyox WSR-301	4000000	0.18 $\pm$ 0.01	130 $\pm$ 1	1.246 $\pm$ 0.002	0.495 $\pm$ 0.005	0.541 $\pm$ 0.009	15.10 $\pm$ 0.36
PEO	Polyox WSR-303	7000000	0.22 $\pm$ 0.06	115 $\pm$ 8	1.246 $\pm$ 0.001	0.473 $\pm$ 0.003	0.548 $\pm$ 0.007	13.68 $\pm$ 0.75
MCC	Avicel PH 200	15–300 [25]	4.03 $\pm$ 0.12	160 $\pm$ 1	1.575 $\pm$ 0.001	0.429 $\pm$ 0.021	0.502 $\pm$ 0.002	14.61 $\pm$ 4.11

### Carr-Index

To analyze flowability the Carr-Index [17] was calculated. It is based on bulk and tap density:

$$\begin{aligned} \text{Carr index} &= \text{compressibility}[\%] = \\ &= \frac{\text{tap density} - \text{bulk density}}{\text{tap density}} 100 \end{aligned} \quad (1)$$

### Glass transition temperature and melting point

The glass transition temperature  $T_g$  was determined using DSC 200 (Netzsch Gerätebau GmbH, Selb, Germany). Hermetically closed pans were used for analysis. Sample size varied between 5 and 10 mg. Heating rate was  $40 \text{ K min}^{-1}$  and only with a high heating rate can weak transitions be determined [18]. The temperature interval was set to  $-80$  to  $150^\circ\text{C}$ . The  $T_g$  was determined by calculating the temperature of the half step height during the first heating. In order to verify the results, additionally the maximum of the first derivative was determined.

The melting point of the materials was determined from the peak set of the DSC trace.

### X-ray diffraction studies

The crystallinities of the powders were compared using a Roentgen diffractometer (URD 63, Freiburger Präzisionsmechanik, Freiberg, Germany). The radiation was copper and a nickel filter was used. Bragg's angle was analyzed between  $3$  and  $50 2\theta$ .

### Compression analysis

#### Tableting

Tableting was performed on an instrumented eccentric tableting machine (EK0/DMS, No. 1.0083.92, Korsch GmbH, Berlin, Germany) with 11 mm diameter flat faced punches (Ritter GmbH, Hamburg, Germany). Equal volumes based on the apparent particle density of the substances were tableted to graded different maximum relative densities ( $\rho_{\text{rel,max}}$ ) of the tablets (precision 0.001) between 0.70 and 0.95 (PEOs: 0.74, 0.79, 0.83, 0.87, 0.92; MCC: 0.72, 0.76, 0.80, 0.84, 0.88). The amount of material necessary for each tablet with a given  $\rho_{\text{rel,max}}$  was calculated. The powder was manually filled into the die; one compaction cycle was performed. The tablet height at maximum densification under load was held constant at 3 mm. Displacement of the punch faces was measured by an inductive transducer (W20 TK, Hottinger Baldwin Meßtechnik, Darmstadt, Germany). Elastic deformation of the punches and the machine was corrected according to [19]. The depth of filling was held constant at 13 mm. The production rate was 10 tablets

per minute. No lubricant was used to avoid its having any influence on the microstructure of the tablets.

Ten single tablets were produced at each condition; data acquisition was performed by a DMC-plus system (Hottinger Baldwin Meßtechnik, Darmstadt, Germany), and data were stored by BEAM-Software (AMS-Flöha, Germany). Force, time, and displacement of the upper punch were recorded for each compaction cycle.

#### Data analysis

For analyzing tableting data only data  $>1 \text{ MPa}$  were used. For five of the ten compaction cycles of each condition normalized time, pressure, and  $\ln(1/1-D_{\text{rel}})$  according to Heckel [20] were calculated.

#### 3D model

For applying the 3D modeling technique [13], all three of the measured values were presented in a 3D data plot. To this 3D data plot a plane twisted at  $t=t_{\text{max}}$  was fitted by the least-squares method according to Levenberg-Marquard (Matlab®):

$$\begin{aligned} z &= \ln\left(\frac{1}{1-D_{\text{rel}}}\right) = \\ &= (t - t_{\text{max}})(d + \omega p_{\text{max}} - p) + ep + (f + dt_{\text{max}}) \end{aligned} \quad (2)$$

with  $D_{\text{rel}}$ =relative density,  $t$ =time,  $p$ =pressure,

$$d = \frac{\delta \ln(1/(1-D_{\text{rel}}))}{\delta t}, \quad e = \frac{\delta \ln(1/(1-D_{\text{rel}}))}{\delta p},$$

$$f = \ln\left(\frac{1}{1-D_{\text{rel}}}\right)$$

$t_{\text{max}}$ =time at maximum pressure,  $p_{\text{max}}$ =the maximum pressure and  $\omega$  = twisting angle at  $t_{\text{max}}$ .

$d$ ,  $e$ , and  $\omega$  of the five compaction cycles at each tableting condition (material and a given  $\rho_{\text{rel,max}}$ ) were averaged, and means and standard deviations were calculated. The mean standard deviation for time plasticity  $d$  was 0.03, for pressure plasticity  $e$  0.0002, and for fast elastic decompression indicated by  $\omega$  it was 0.0006.

#### Heckel function

Heckel describes the decrease of porosity with pressure by first order kinetics [20].

$$-\ln \varepsilon = \ln\left(\frac{1}{1-D_{\text{rel}}}\right) = Kp + A \quad (3)$$

with  $\varepsilon$ =porosity,  $D_{\text{rel}}$ =relative density,  $K$ =slope of the Heckel equation,  $p$ =pressure, and  $A$ =point of intersection with the y-axis.

The Heckel equation is applicable at the compression part of a porosity pressure plot. A linear fit was performed with an accuracy of  $R=0.999$  and better. The fit included as much data from the compression part as possible which was determined by iteration.

The slope of the Heckel equation gives information on the total deformation of the powder.

#### Pressure time function

The pressure-time-function is a repeatedly modified Weibull equation [21].

$$p(t) = p_{O_{\max}} \left[ \frac{t_{\text{end}} - t}{\beta} \right]^{\gamma} e^{-1 \left[ \frac{t_{\text{end}} - t}{\beta} \right]^{\gamma}} \quad (4)$$

with  $p(t)$ =pressure,  $p_{O_{\max}}$ =maximum pressure of the upper punch,  $t$ =time,  $t_{\text{end}}$ =time at the lifting of the upper punch,  $\beta$ =time difference between the maximum pressure and the lifting of the upper punch, and  $\gamma$ =parameter of asymmetry of the plot.

In the present form it is able to describe the normalized pressure-time-curve of the tableting process. The parameter  $\gamma$  indicates the symmetry of the plot and is a measure for the elasticity of the powder, hence with increasing  $\gamma$  elastic deformation increases. The parameter  $\beta$  is the time difference between maximum pressure and the lifting of the upper punch from the tablet. Information on the elastic recovery during tableting is given.

$\gamma$  and  $\beta$  can be presented in a  $\gamma$ - $\beta$ -diagram which gives information on the deformation behavior of the powders. In this study, the mean standard deviation for  $\gamma$  was 0.03, and for  $\beta$  it was 1.01.

#### Force-displacement-profiles

Force-displacement-profiles are used to calculate the different types of energy used for tableting [22]. The analysis includes the compression and decompression of the powder to the tablet. The area between compression and decompression is called the area of compaction energy. The area between maximum displacement and decompression is the elastic energy. Both these types of energy were calculated for five compaction cycles, mean and standard deviations were calculated.

#### Elastic recovery

Elastic recovery after tableting was calculated according to Armstrong and Haines-Nutt [23]:

$$ER(\%) = 100 \frac{H_1 - H_0}{H_0} \quad (5)$$

with  $ER$ =elastic recovery,  $H_1$ =height of the tablet after 10 days, and  $H_0$ =minimal height of tablet under load.

The calibrated inductive transducer (W 20 TK, Hottinger Baldwin Meßtechnik, Darmstadt, Germany) was used to measure the axial expansion in the die. The height of the tablet after 10 days was measured by a micrometer screw (Mitotuyo, Tokyo, Japan). Ten tablets were analyzed, and the means and standard deviations were calculated.

Additionally, elastic recovery was determined in dependence on time [24].

#### Crushing force

The crushing force of the tablets was analyzed with the crushing force tester (TBH 30, Erweka GmbH, Heusenstamm Germany) using a compression rate of  $2.3 \text{ mm s}^{-1}$  during the crushing force test. For each condition, five tablets were analyzed 10 days after tableting. Means and standard deviations were calculated.

## Results and discussion

### Material properties

Figure 1 exhibits the sorption isotherms of the five different PEOs when compared to MCC. For all of them the water sorption is lower than the water sorption of MCC. Up to 50% RH there is hardly any influence of relative humidity visible and no influence of molecular mass can be detected. During the storage interval between 35 and 45% RH water sorption was detected to be less than 0.2% (mass/mass). Thus, when comparing the five PEOs under the conditions used, any influence, that RH has, can be deemed insignificant. Furthermore, Table 1 shows that the water content of the materials as determined by thermogravimetry ranges from 0.18–0.33% (mass/mass). The lower molecular masses tend to sorb slightly more water, however considering standard deviation the differences are insignificant. The water content

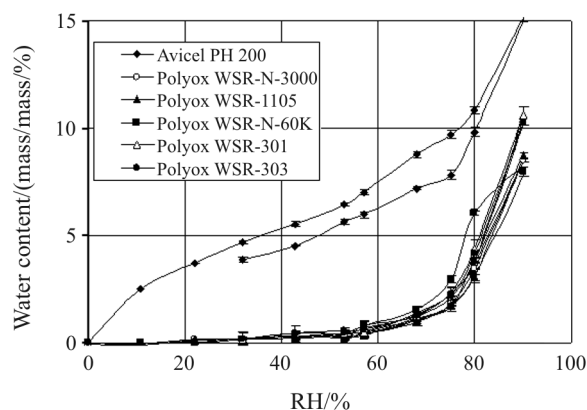


Fig. 1 Sorption isotherms of different PEOs when compared to MCC



measured by TG corresponds with the water content measured during sorption. It can, therefore, be stated that when RH increases above 50%, the PEOs adsorb water at a stronger rate and this is also the case for the higher molecular masses.

Figure 2 shows the cumulative particle size distribution. Particle size is similar for all five PEOs, except for P303, which is slightly lower. However as Table I shows the standard deviation for the median particle size of P303, which is 8-fold that of the other PEOs. Considering this fact it can be assumed that this difference in particle size is of minor importance. For all of the materials, bulk samples were used and thus, the differences as reported by Yang *et al.* [9] will not influence the results. In comparison to the PEOs, Avicel PH 200 was used with a particle size which is about 20  $\mu\text{m}$  higher. This was the MCC bulk material which was available with the most similar particle size. Thus, overall, when comparing material deformation behavior, the influence of particle size is of little importance.

The particle shape of the powders is shown exemplarily for P60K and P303 in Fig. 3. The particles are smooth edged but irregular in shape. At higher magnification they appear to consist of a lot of fine particles.

In Table 1 the apparent particle, tap and bulk density of the materials are given. Apparent particle density is similar for that of the PEOs with different molecular masses and it is in accordance with the literature [9, 10]. Bulk and tap density of the PEOs can be divided in two groups: P3000 and P1105; those with a molecular mass below 1.000.000 Da show a

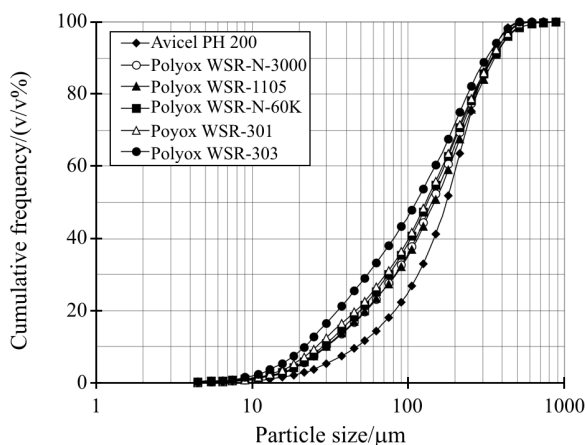


Fig. 2 Particle size determined by laser diffraction of different PEOs and MCC

higher bulk and tap density than the three other PEOs with a molecular mass above 1.000.000 Da.

Bulk and tap density can give information on the flowability of the powders and using both these values the Carr index was calculated. According to Carr [17], a value of 5–10, 12–16, 18–21 and 23–28 represent excellent, good, fair, and poor flow properties. Thus flowability of the PEOs was good and furthermore, it is similar to the special type of MCC used in this study. These results are in accordance with Yang *et al.* [9] but not with Efentakis and Vlachou [11].

As it has already been established, the deformation of materials is dependent on their  $T_g$ . For the different types of PEO, the  $T_g$ s were determined to be:  $-41.0 \pm 12.8$  (P3000),  $-36.8 \pm 13.5$  (P1105),  $-43.0 \pm 8.5$  (P60K),  $-50.6 \pm 0.9$  (P301),  $-29.8 \pm 1.1$  (P303), which

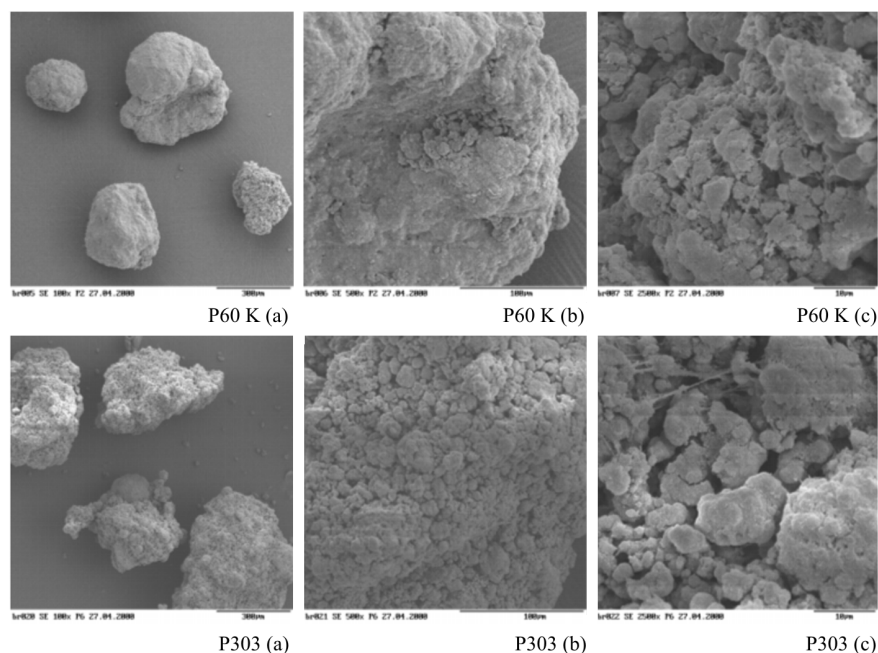


Fig. 3 SEM of powders of Polyox WSR-N-60K and Polyox WSR-303, at a – 100 $\times$ , b – 500 $\times$ , and c – 2500 $\times$  magnification

is in accordance with the literature [8]. The results revealed no order with regards to molecular mass. However, it can be stated that the PEOs are definitely in the rubbery state during tableting.

In addition, the melting point of all PEOs was determined to be between 65 and 69°C.

*Tableting*

The tableting behavior was characterized by the following: 3D modeling (Figs 4 and 5) in comparison to the Heckel analysis (Fig. 6a), determination of the parameters of the pressure time function (Fig. 6b), and energy calculations from the force-displacement-profile (Figs 6c and d).

Figure 4a shows two different types of PEO, namely P3000 and P303, when compared to MCC and when analyzed by 3D modeling. The PEOs show a strongly higher pressure plasticity  $e$  than MCC and

fast elastic decompression indicated by  $\omega$  is also higher when compared to MCC. Time plasticity  $d$  is only slightly higher than that of MCC. Thus they are much more ductile than MCC and also more ductile than most other materials which have been already analyzed by 3D modeling [13, 14].

The molecular mass of the PEOs increases in the following order: P3000<P1105<P60K<P301<P303. The  $d$ -values of the five PEOs are within standard deviation (Fig. 5a): for the  $\omega$ -values no order could be derived (Fig. 5c), however, for the  $e$ -values the following order was set up:  $e(\text{P3000}) > e(\text{P301}) > e(\text{P1105}) > e(\text{P60K}) > e(\text{P303})$  (Fig. 5b). Since the standard deviation is as low as 0.0002, a decrease in  $e$ -values with the exception of P301 occurs after an increase in molecular mass (Fig. 4b). Hence it can be concluded that there is a weak association between deformation behavior and molecular mass. This is

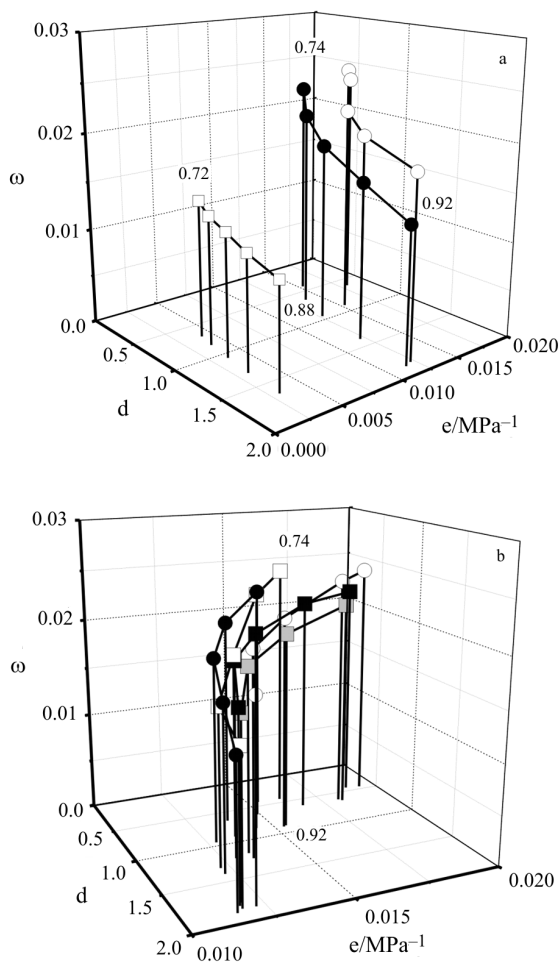


**Fig. 4** 3D parameter plot in dependence on  $\rho_{\text{rel,max}}$  (0.72–0.92) of a –  $\square$  – Avicel PH 200,  $\bullet$  – Polyox WSR-303,  $\circ$  – Polyox WSR-N-3000 and b –  $\bullet$  – Polyox WSR-303,  $\blacksquare$  – Polyox WSR-301,  $\square$  – Polyox WSR-N-60K, grey  $\square$  – Polyox WSR-1105,  $\circ$  – Polyox WSR-N-3000

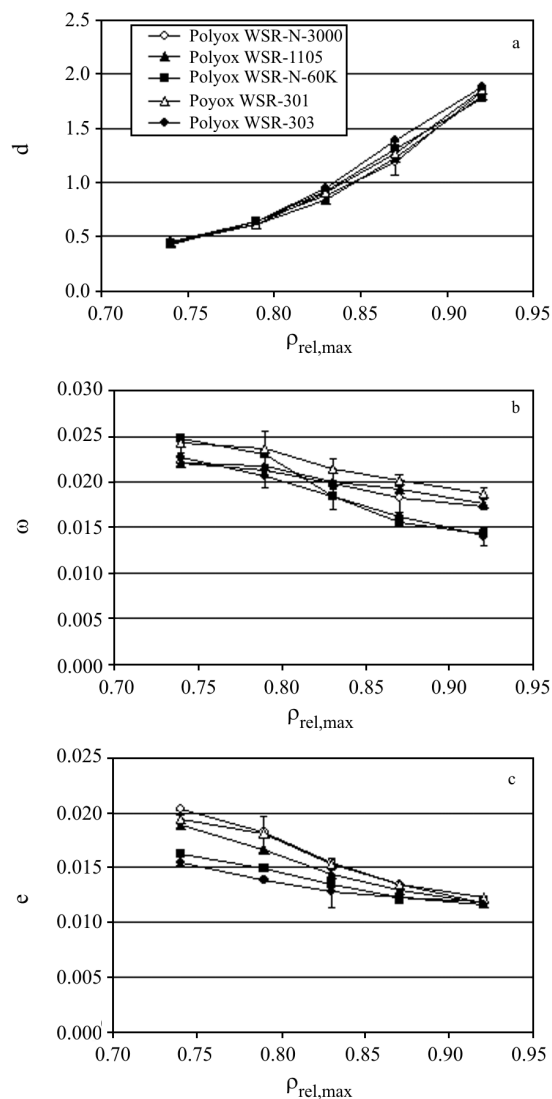


**Fig. 5** Parameters of the 3D model in dependence on  $\rho_{\text{rel,max}}$  of the PEOs: a –  $d$ -values, b –  $e$ -values and c –  $\omega$ -values

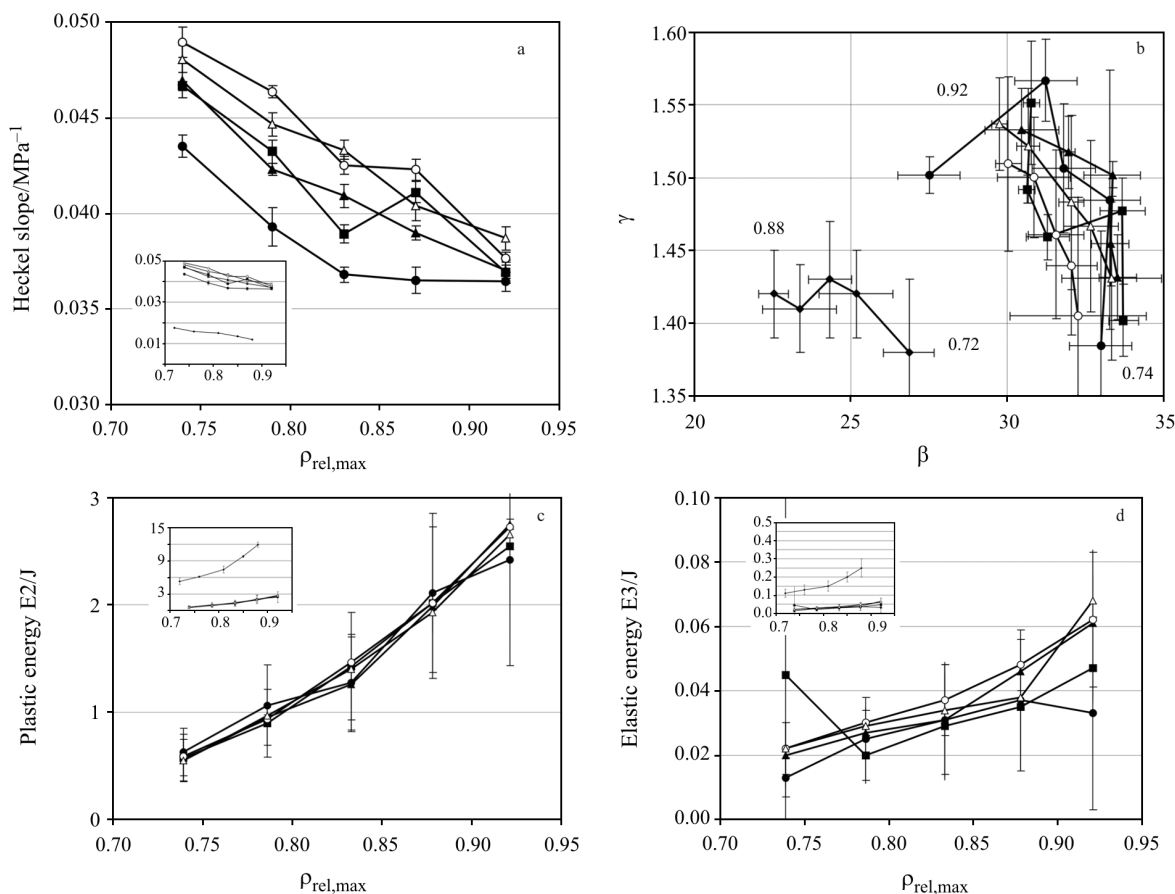


**Fig. 6** a – Heckel slope, b –  $\beta$ - $\gamma$ -diagram, c – plastic and d – elastic energy in dependence on  $\rho_{rel,max}$  determined for different PEOs: ● – Polyox WSR-303,  $\triangle$  – Polyox WSR-301, ■ – Polyox WSR-N-60K, ▲ – Polyox WSR-1105, ○ – Polyox WSR-N-3000 and compared with MCC (small diagram)

contrary to Yang's *et al.* results [9], who reported that there is no influence of molecular mass.

Figure 5a shows the slope of the Heckel function for the different PEOs. All of the PEOs exhibited a higher slope of the Heckel function than MCC. This indicates that the PEOs are much more ductile than MCC which has already been analyzed by 3D modeling. When taking standard deviation into account, the following order for the slope of the Heckel function can be set up:  $k(\text{P3000}) \approx k(\text{P301}) > k(\text{P60K}) \approx k(\text{P1105}) > k(\text{P303})$ . No dependency of deformation on molecular mass could be detected, which is in agreement with [9]. Contrary to pressure plasticity  $e$  of the 3D model the determination of the Heckel slope includes plastic and elastic deformation which makes the analysis much less precise.

Figure 6b shows the results of the analysis with the pressure-time function in the  $\beta$ - $\gamma$ -diagram. All PEOs exhibit higher  $\beta$ - and  $\gamma$ -values than MCC which is an indication of elastic deformation. Considering standard deviation, no differences between different molecular masses of PEO are visible. However, compared to Heckel analysis and pressure plasticity  $e$ , it can be assumed that this is time dependent deforma-

tion. The result is in agreement with the time plasticity  $d$  from 3D modeling.

Finally, Figs 6c and d exhibit compaction and elastic energy which were determined from force-displacement-profiles; compaction energy is the net energy which remains in the tablet [22]. Elastic energy is the energy released during decompression. Moreover, compaction and elastic energy are much lower for the PEOs than for MCC which means that less energy is needed for deformation. Considering standard deviation, plastic and elastic energy are the same for all PEOs even if they are of different molecular mass.

To sum up, molecular mass has no detectable influence on tablet formation when the Heckel analysis, analysis by the pressure-time-function and energy analysis using force-displacement-profiles are used. On the contrary 3D modeling is able to differentiate: a time-dependent influence of molecular mass and differences in elasticity during compression do not exist, however a weak pressure dependent influence is visible with pressure plasticity  $e$ . Thus 3D modeling is able to differentiate in one step between time dependent and pressure dependent deformation.



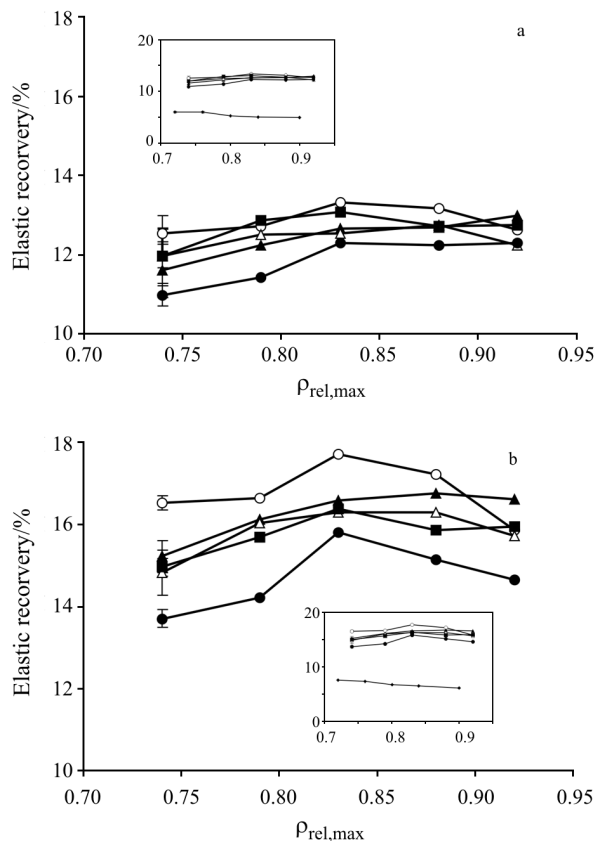


**Fig. 7** Elastic recovery in dependence on  $\rho_{rel,max}$  of different PEOs (● – Polyox WSR-303, △ – Polyox WSR-301, ■ – Polyox WSR-N-60K, ▲ – Polyox WSR-1105, ○ – Polyox WSR-N-3000) and compared with MCC (small diagram): a – directly after tableting and b – ten days after tableting

#### Final formation of the tablets

Firstly, elastic recovery after tableting was analyzed in dependence on time (data not shown). A slight and

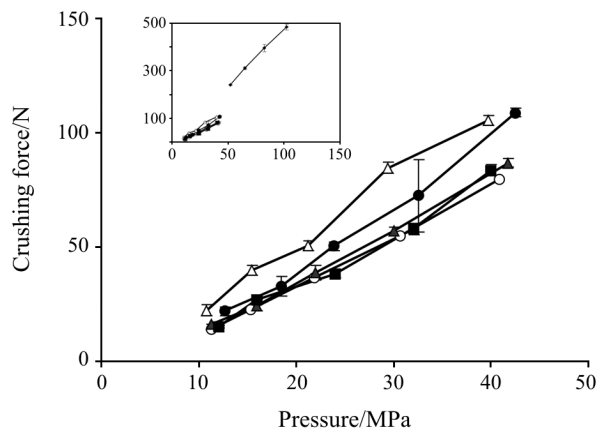


**Fig. 8** Compactibility plot of different PEOs (● – Polyox WSR-303, △ – Polyox WSR-301, ■ – Polyox WSR-N-60K, ▲ – Polyox WSR-1105, ○ – Polyox WSR-N-3000) and compared with MCC (small diagram)

continuous increase of tablet height could be detected. No shrinking of the tablets occurred as with MCC and carrageenan [24].

Figure 7 shows the elastic recovery of the different PEO tablets in dependence on  $\rho_{rel,max}$  compared to MCC. Elastic recovery is higher than for the MCC tablets. Relaxation which already started during tableting continues. For elastic recovery of the PEOs with different molecular mass no concrete order could be set up and thus elasticity after tableting remains the same. This result is in agreement with Yang *et al.* [9]. In summation, a great deal of the tablet formation process continues after tableting. The PEOs which deformed elastically and plastically during tableting expand much more than MCC after tableting.

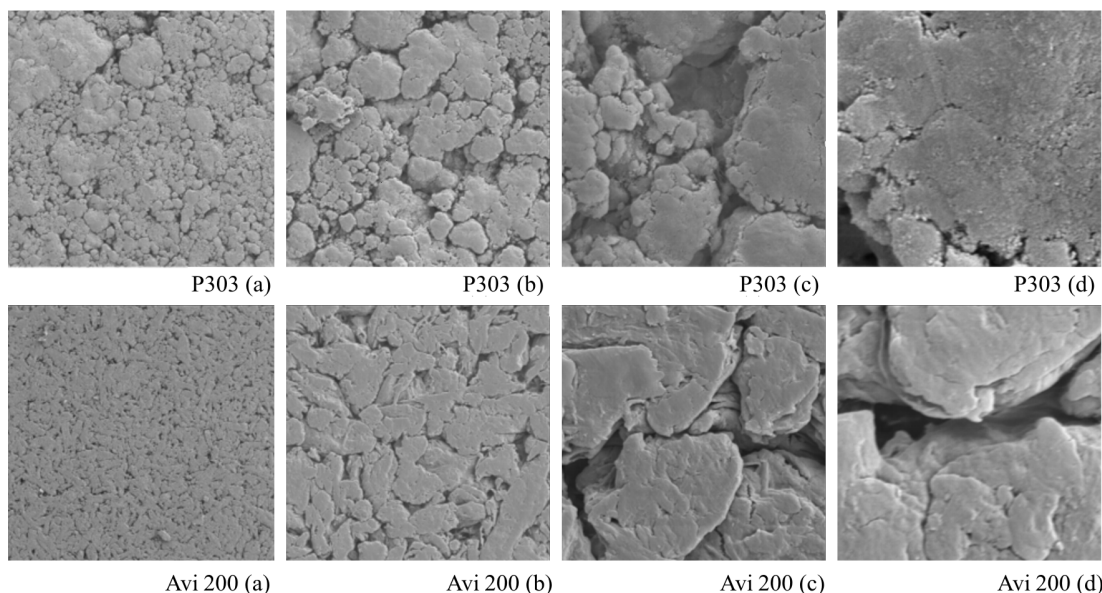
#### Tablet properties

Figure 8 shows the compactibility of the PEOs when compared to MCC. PEOs show a very low compactibility. The high level of relaxation after tableting as shown by elastic recovery might contribute to the low strength of the compacts. Furthermore, as it has already been shown, the  $T_g$  of the PEOs is as low as  $-30$  to  $-50^\circ\text{C}$ . The materials are in the rubbery state during and after tableting. No reversible exceeding of the  $T_g$  is possible during tableting [21] which could improve the formation of bonds between the particles. P301 and P303 with a higher molecular mass showed a slightly higher compactibility than the other three PEOs, which behave in a similar fashion. Overall, no order for the influence of molecular mass could be set up.

Figure 9 exhibits an example for the upper surface of a PEO tablet after tableting and relaxation as analyzed by SEM. The surface appears rough and a great number of gaps is visible. This is contrary to MCC (Avi 200). For MCC, the tablet surface appears smooth and the particles are strongly deformed. In conclusion, easy deformation of the particles during tableting as for the PEOs is no guarantee for mechanically stable tablets.

#### Conclusions

The PEOs are in the rubbery state during tableting. This might be one reason why they are much more easily deformable than MCC and more than most other excipients [12–14]. Differences between the different types are slight, however, when using the recently introduced 3D modeling technique, a weak association between pressure dependent deformation and molecular mass could be detected. This difference was not visible when other more traditional techniques were used. Moreover, the predominant ductility during deformation of the PEOs can be attributed



**Fig. 9** SEM of the surface of tablets of Polyox WSR-303 and Avicel 200 at a – 100×, b – 500×, c – 2500× and d – 10000× magnification

to their very low  $T_g$  because only low energy is needed to form a tablet. This tablet in question relaxes slowly after tableting and the formed tablets exhibit a low crushing force. In conclusion, compactibility is low and hence the mechanical stability of the tablets is not sufficient.

### Acknowledgements

The author gratefully acknowledges Union Carbide Inc. for donation of the PEOs. I would also like to thank Dr.-Ing. K. Legenhausen of the Institute of Mechanical Engineering, Technical University Clausthal-Zellerfeld, for permitting the use of laser light diffractometry equipment.

### References

- 1 C. J. Kim, *J. Pharm. Sci.*, 84 (1995) 303.
- 2 C. J. Kim, *Drug Dev. Ind. Pharm.*, 24 (1998) 645.
- 3 L. Maggi, R. Bruni and U. Conte, *Int. J. Pharm.*, 195 (2000) 229.
- 4 J. F. Pinto, K. F. Wunder and A. Okolockwe, *AAPS PharmSci*, 6 (2004) article 15.
- 5 A. Apicella, B. Cappello, M. A. Del Nobile, M. I. La Rotonda, G. Mensitieri and L. Nicolais, *Biomaterials*, 14 (1993) 83.
- 6 A. G. Schmidt, S. Wartewig and K. M. Picker, *J. Raman Spectr.*, 35 (2004) 360.
- 7 J. Falbe and M. Regitz, *Römpp Chemie Lexikon*. Thieme Verlag, Stuttgart, 1995.
- 8 J. V. Koleske, Poly(ethylene oxide) (Overview), in: Salomone, J. C. (Ed.), *Polymeric Materials Encyclopedia*, CRC Press Inc., Electronic release, 1996.
- 9 J. Yang, G. Venkatesh and R. Fassihi, *J. Pharm. Sci.*, 85 (1996) 1085.
- 10 F. E. Bailey and J. V. Koleske, Polyoxyalkylenes, in: *Ullmann's Encyclopedia of Industrial Chemistry*, Electronic release, 2000.
- 11 M. Efentakis and M. Vlachou, *Pharm. Dev. Technol.*, 5 (2000) 339.
- 12 K. M. Picker, *Eur. J. Pharm. Biopharm.*, 49 (2000) 267.
- 13 K. M. Picker, *Drug Dev. Ind. Pharm.*, 30 (2004) 413.
- 14 K. Hauschild and K. M. Picker-Freyer, *AAPS PharmSci*, 6 (2004) article 16 .
- 15 L. Greenspan, *J. Res. Nat. Bur. Stand.*, 81A (1977) 89.
- 16 K. M. Picker and J. B. Mielck, *Eur. J. Pharm. Biopharm.*, 42 (1996) 82.
- 17 R. L. Carr, *Chem. Eng.*, 72 (1965) 163.
- 18 K. M. Picker, *J. Therm. Anal. Cal.*, 73 (2003) 597.
- 19 M. Krumme, L. Schwabe and K. H. Frömming, *Acta Pharm. Hung.*, 68 (1998) 322.
- 20 R. W. Heckel, *Trans. Metall. Soc. AIME*, 221 (1961) 1001.
- 21 R. Dietrich and J. B. Mielck, *Pharm. Ind.*, 47 (1985) 216.
- 22 M. Dürr, D. Hanssen and H. Harwalik, *Pharm. Ind.*, 34 (1972) 905.
- 23 N. A. Armstrong and R. F. Haines-Nutt, *J. Pharm. Pharmacol.*, 24 S (1972) 135.
- 24 K. M. Picker, *Pharm. Dev. Technol.*, 6 (2001) 61.
- 25 O. A. Battista, D. Hill and P. A. Smith, Level-off D.P. cellulose products, US Patent 2,978,446 (1961).

DOI: 10.1007/s10973-006-7698-8